Journal Pre-proofs

Preparation and FTIR, Raman and SEM characterizations of Konjac Glucomannan-KCl electrogels

Li-Xia Wang, Anng-Ruei Lee, Yi Yuan, Xiu-Mei Wang, Ting-Jang Lu

PII: S0308-8146(20)31151-1
DOI: https://doi.org/10.1016/j.foodchem.2020.127289
Reference: FOCH 127289

To appear in: *Food Chemistry*

Received Date: 20 August 2019
Revised Date: 28 May 2020
Accepted Date: 7 June 2020

Please cite this article as: Wang, L-X., Lee, A-R., Yuan, Y., Wang, X-M., Lu, T-J., Preparation and FTIR, Raman and SEM characterizations of Konjac Glucomannan-KCl electrogels, *Food Chemistry* (2020), doi: https://doi.org/10.1016/j.foodchem.2020.127289

Preparation and FTIR, Raman and SEM characterizations of Konjac Glucomannan-KCl electrogels

Li-Xia Wang [a, b, c], Anng-Ruei Lee [b], Yi Yuan[d], Xiu-Mei Wang [a], Ting-Jang Lu [b, *]

[a] *School of Environmental and Biological Engineering, Putian University, Putian 351100, China*

[b] *Graduate Institute of Food Science and Technology, Taiwan University, No.1, Sec.4, Roosevelt Road, Taipei 10617, Taiwan, ROC*

[c] *Fujian Provincial Key Laboratory of Ecology-Toxicological Effects & Control for Emerging Contaminants, Putian University, Putian 351100, China*

[d] *School of Food Science and Engineering, South China University of Technology, Guangzhou 510641, China*

ABSTRACT

Konjac glucomannan (KGM) electrogels were successfully prepared under alternating current (AC) in the presence of potassium chloride (KCl). The structure of the gels was studied using Fourier transform infrared spectroscopy (FTIR), Raman spectroscopy, and scanning electron microscopy (SEM). A single-factor experiment was performed to optimize the preparation of the gels. Our results showed that KGM was degraded under AC and partially deacetylated. KGM and KCl formed the structure 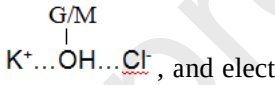

, and electrogels with porous structures retained some acetyl groups. Furthermore, as the KCl concentrations, voltages, time, and KGM concentrations increased, the viscoelastic moduli of the gels increased; the moduli decreased when the KCl concentrations, voltages, and time exceeded critical values.

Keywords: Konjac Glucomannan (KGM); Potassium chloride (KCl); Alternating current (AC) electric field; Gel; Structural characterization; Preparation conditions

1. Introduction

Gels are used widely in food products and packaging films, and they are used as additives, matrices, and pharmaceutical and nutrient carriers (Niu, Xia, Li, Wang, & Yu, 2019; Luo, Teng, Wang, & Wang, 2013). The major factor defining the properties of gels is the preparation method, which also determines their applications. Konjac glucomannan (KGM) is a naturally occurring neutral polysaccharide extracted from *Amorphophallus konjac* C. Due to its good film and gel formation capacity, biocompatibility and biodegradability, KGM has been used in the food, medical, environmental, biotechnical and material fields (Zhang, Xie, &Gan, 2005; Zhu, 2018).

For instance, it can form thermally irreversible gels in the presence of an alkaline coagulant (Zhou, Jiang, Perkins, & Cheng, 2018). Alkali facilitates deacetylation and decreases the solvation of KGM chains. KGM transits from random coil configurations to more stiff configurations accompanied by self-assembly to aggregate with one another and form junction zones. The molecular forces responsible for gel formation are thought to be hydrogen bonding and hydrophobic interactions. KGM can also form thermally reversible gels with borate (Gao, Guo, & Nishinari, 2008). The gel network is formed through the crosslinking reaction between borate ions and the *cis*-diol hydroxyl groups on the mannose units of KGM chains. However, boron ions are toxic and non-food grade, which greatly limits the practical applications of the gel in food. KGM could also form reversible complex gels with other polysaccharides or proteins, such as xanthan, carrageenan, and agarose, through intermolecular hydrogen interactions and synergistic effects (Brenner, Tuvikene, Fang, Matsukawa, & Nishinari, 2015). Furthermore, a novel low-alkali alcogel was prepared by mixing ethanol with KGM aqueous solution containing a

certain concentration of Na_2CO_3 (Zhou, Wu, Tian, Li, Zhu, Zhao, & Cheng, 2020). The use of alcohol as an antisolvent reduced the solubility of the KGM solute and resulted in the rapid precipitation of the solute or, in some special cases, gelation. Our team previously utilized low-voltage direct current (DC) to induce the formation of KGM electrogels in the presence of tungstate ions. The preparation parameters, rheological properties, and texture properties of these gels were studied, and a mechanism for formation was proposed (Wang, Jiang, Lin, Pang, & Liu, 2016; Wang, Zhuang, Li, Pang, & Liu, 2016).

It has been reported that AC can control the orientation of molecules or create crosslinking by dielectrophoresis forces. For instance, Zhuo Chen et al. (2005) demonstrated controllable interconnections of single-walled carbon nanotubes between two electrodes under AC (2.5×10^5 V/m, 5 MHz), and the interconnected carbon nanotubes were parallel with the electric flux. Hermanson et al. (2001) reported that metallic nanoparticles could assemble into microwires in aqueous suspension by dielectrophoresis, and then, the nanoparticles aggregate to extend the wire in the direction of the field gradient with an alternating voltage (50 to 250 V, 50 to 200 Hz) applied to the planar electrodes (resulting in a field intensity of ~250 V/cm). However, these studies focused on the assembly or aggregation of small molecules driven by AC with high voltage or high frequency. Whether AC can induce the reorientation, crosslinking, or aggregation of biomacromolecules, such as KGM, to form gels has not been reported. Based on the reports that AC can induce the aggregation of small molecules and our previous research on KGM-tungsten gels induced by DC, we examined the potential of fabricating a new KGM electrogel under AC. Thus, the aim of this study was to utilize an AC electric field to induce KGM to self-assemble into three-dimensional gel networks and examine the structural and rheological characteristics of the gels.

2. Materials and methods

2.1. Materials

KGM powder was purchased from Sanai Konjac Biotechnology Co., Ltd. (Zhaotong, China). KCl was analytical grade and purchased from Cuilin Huabo Instrument Co., Ltd. (Zhangzhou, China).

2.2. Preparation of KGM-KCl electrogel under AC electric field

KGM-KCl electrogels were prepared according to Wang et al. (2016) with some modifications. Briefly, 0.5 ~ 0.9% KCl was added to KGM hydrosol (0.5~1.1%). Carbon rods were inserted into the mixture, and an AC (21~25 V) was applied for at least 35 min. The distance between the two rods was fixed at 4 cm. Optimal gel formation was achieved using a mono-factor experiment, using elastic modulus as the evaluation parameter.

2.3. Fourier transform infrared (FTIR) spectroscopy

FTIR spectra of KGM powder, lyophilized KGM hydrosol treated by an AC electric field for a certain time (KGM-AC) and frozen-dried gel samples were recorded on a Nicolet iS10 FTIR spectrometer (Thermo Fisher Scientific Inc., WI, USA) in the range of 400 - 4000 cm^{-1}.

2.4. Raman spectroscopy

Raman spectra were recorded with a Labram Aramis confocal microprobe analyser (Horiba Jobin-Yvon, Longjumeau, France) equipped with an Olympus microscope and a CCD cooled according to Wang, Jiang, Lin, Pang and Liu (2016).

2.5. Scanning electron microscopy (SEM)

KGM powder, lyophilized KGM hydrosol, lyophilized KGM hydrosol treated by an AC electric field for a certain time (KGM-AC) and lyophilized KGM-KCl gels were attached to the aluminium plate through double-sided conductive carbon tabs. After being coated with gold in an SCD-500 ion sputter (Hitachi Ltd., Hitachi, Tokyo, Japan), the samples were observed by a Quanta250/Qunta430 Thermal Field Emission Scanning Electron Microscope (FEI Co., Hillsboro, OR, USA).

2.6. Rheological measurements

Steady flow measurements and dynamic oscillatory tests were performed on an AR-2000 ex stress-controlled rheometer (TA Instrument, New Castle, DE, USA) equipped with a Peltier device for temperature control using a plate-plate geometry (diameter 40 mm for sol samples, 20 mm for gel samples, gap 0.2 mm). KGM and KGM-KCl sols were loaded on the plate, allowed to equilibrate at 25 ℃ for 2 min, and then subjected to increasing shear rates from 1 to 200 s^{-1} (Wang, Xiong, & Sato, 2017). The apparent viscosity (η_a) was recorded as a function of shear rate. The fresh gel samples were also equilibrated at 25 ℃ for 2 min before rheological measurements. The linear viscoelastic region (LVR) for gel samples was determined by performing amplitude sweep measurements (0.01-5%) at constant frequency (1 Hz) and 25 ℃. Frequency sweep tests at a constant strain of 0.5% were carried out to determine the viscoelastic nature of the KGM-KCl electrogel. Under this strain limit, the gel network structure will not be destroyed by the measurements. All measurements were performed at least in triplicate.

3. Results and discussion

3.1. Preparation of KGM-KCl electrogel under AC electric field

When an AC electric field was applied on a certain volume of 0.5% KGM hydrosol, no gel formation was observed, even with an electric treatment of 45 min. There was also no heat release phenomenon or gas production during the course of electric treatment. No gel formed when KGM hydrosol contained sodium tungstate treated by AC. However, white gels were produced at the gas/liquid interface when AC was utilized to process 0.5% KGM hydrosol containing a certain amount of KCl. Moreover, bubbles were produced, and heat was released during the treatment. The bubbles were ascribed to the production of H^+ and OH^- from water electrolysis during the course of electric treatment, resulting in the release of hydrogen and oxygen gases. It also occurred in the process of water electrolysis caused by a DC (Wang, Zhuang, Li, Pang, & Liu, 2016). Heat release was due to the violent movement of ions in the AC electric field. It should be noted that when the KCl concentration was above 0.9%, no gel formed. At this time, the KGM hydrosol began to boil, and its fluidity increased under high temperature caused by ion movements. In addition, it can be observed that the KGM sol became thinner, as KGM could not withstand temperatures above 80 ℃ (Wang, Jiang, Lin, Pang, & Liu, 2016). Therefore, a suitable concentration of KCl was necessary for the formation of KGM electrogels under an AC electric field. On the other hand, when the voltage applied was below 21 V or above 26 V, there was also no gel formation, indicating that the application of a suitable voltage was another important factor that determined the gel formation. Overall, an appropriate KCl concentration and voltage are essential conditions for the formation of KGM electrogels.

3.2 FTIR spectroscopy

FTIR spectra of native KGM powder, KGM-AC and KGM-KCl gel are shown in Fig. 1. The strong absorption at 3346.99 cm^{-1} corresponded to the stretching vibration of -OH. The peak at 2884.14 cm^{-1}

corresponded to the C-H stretching vibrations in the $-CH_2$ or $-CH_3$ groups. The stretching vibration of the carbonyl at 1724.12 cm^{-1} corresponded to characteristic acetyl groups of KGM molecules (Li, Ma, Chen, He, & Huang, 2018). The absorption band at 1640.23 cm^{-1} corresponded to the C-O stretching vibrations related to -OH (Ye, Jin, Huang, Hu, Li, Li, & Li, 2017). The absorption peak at 1022.13 cm^{-1} corresponded to C-O-C vibrations (Li, Ji, Li, Zhang, Xiong, & Sun, 2017). The absorption peaks at 898.70 cm^{-1} and 805.65 cm^{-1} corresponded to the stretching vibrations of mannose units (Wang, Wu, Xiao, Kuang, Corke, Ni, & Jiang, 2017).

As shown in Fig. 1, some differences were found among the spectra. The chemical structures of KGM-AC and KGM-KCl electrogel were similar to that of native KGM. When compared with the spectrum of native KGM, the peak at 3358.42 cm^{-1} in KGM-AC became distinctly weaker and wider, indicating that the -OH vibrations were affected. In addition, the peak in native KGM at 3346.99 cm^{-1} shifted to a higher frequency of 3358.42 cm^{-1} in KGM-AC, which could be attributed to the complex vibrational stretches associated with free, inter- and intramolecular hydroxyl groups (Wang, Zhou, Wang, & Li, 2015). The higher the peak frequency was, the weaker the interaction was (Sun, Li, Dai, Ji, & Xiong, 2014). Li et al. also reported that the characteristic bands at 3500-3300 cm^{-1} of short linear glucan (SLG) nanoparticles shifted to a lower wavelength in SLG/soy protein isolate (SPI) nanoparticles, indicating that the interaction force of intermolecular hydrogen bonds between SLG and SPI molecules was enhanced (Li, Ji, Li, Zhang, Xiong, & Sun, 2017). These results all showed that the vibration of -OH in KGM-AC was affected. Meanwhile, the peak at 1022.13 cm^{-1} in native KGM shifted to a higher frequency of 1025.46 cm^{-1} in KGM-AC and became weaker, suggesting the breaking of glycosidic bonds (Wang, Zhou, Wang, & Li, 2015). From the above analysis, we could conclude that KGM degraded under an AC electric field. In addition, the stretching peak of the carbonyl at 1724.12 cm^{-1} in KGM-AC decreased, indicating that the characteristic acetyl groups of KGM molecules decreased; this decrease might have been due to a certain degree of deacetylation by hydroxide ions, which derived from water electrolysis.

However, the peaks of -OH and C-O-C stretching vibrations in the KGM-KCl gel strengthened again. It is plausible that electrostatic rejection and electrostatic attraction resulting from K^+ and Cl^{-1} on hydroxyl groups might be responsible for the strengthening of the vibration. The interactions between hydroxyl and ions included oxygen atoms of hydroxyl groups interacting with metal ions and hydrogen atoms having a weak interaction with anions to form the structure of M^{n+}…OH…$anion^{n-}$. The interactions between the hydroxyl groups of citrus pectin and monovalent cations, such as Na^+ and K^+, were also elucidated by Wang et al. (Wang, Wan, Chen, Guo, Liu, & Pan, 2019). In our system, hydroxyl groups of KGM molecules interacted with K^+ and Cl^- to form the structure of $\begin{matrix} G/M \\ | \\ K^+\ldots OH\ldots Cl^- \end{matrix}$. G represents glucose, and M represents mannose. Thus, the hydrogen bond interactions in the gel were decreased. Combined with the fact that the gel formed at the gas/liquid interface, we believed that the main forces of gel formation were electrostatic and hydrophobic interactions instead of hydrogen bonds.

The stretching peak of the carbonyl at 1724.12 cm^{-1} indicated that the characteristic acetyl groups of KGM molecules remained in the KGM-AC and KGM-KCl electrogels. No new characteristic peaks appeared in KGM-AC and KGM-KCl gels, indicating that AC electric field treatment did not change the main structure of KGM molecules or produce new functional groups.

3.3 Raman analysis

Fig. 2 shows Raman spectra for KGM powder, KGM-AC and KGM-KCl electrogel in the wavenumber range of 0-3500 cm^{-1}. The weak band at 3360.18 cm^{-1} corresponded to the O-H stretching vibration (Mu et al., 2018). The strong band at 2888.84 cm^{-1} corresponded to the C-H stretching modes (Zhang, Yang, Xu et al., 2018). The weak peak at 1657.72 cm^{-1} corresponded to the vibration of carbonyl (C=O), and the peak at 1453.71 cm^{-1} corresponded to the vibration of methyl ($-CH_3$) in the acetyl group (Jian, Siu, & Wu, 2015). The bands at 1117.38 cm^{-1} and 1085.27 cm^{-1} corresponded to the C-O-C vibration from the glycosidic bonds of KGM molecules (Mu et al., 2018).

In comparison with the Raman spectra of KGM and KGM-AC, almost all the typical characteristic peaks were weakened. The peaks at 1124 cm^{-1} and 1084.32 cm^{-1} decreased, indicating that the vibration of C-O-C in KGM-AC was affected. That is, the glycosidic bonds broke. In addition, -OH, C-H and C=O vibrations also decreased in the spectrum of KGM-AC, suggesting that KGM degraded under an AC electric field and partially deacetylated due to the increase in local hydroxide ion concentration.

The O-H vibrational band at 3360.18 cm^{-1} recovered in the spectrum of the KGM-KCl gel, which could be explained as the result of electrostatic interactions induced by the adsorption of K^+ and Cl^- ions on hydroxyl groups of KGM (Wang, Shen, Liu et al., 2018). This explanation is supported by Qiang Sun and his collaborator. They investigated the interactions among monovalent and divalent cations, chloranion and water in NaCl-H_2O, KCl-H_2O, $CaCl_2$-H_2O, $MgCl_2$-H_2O and NaCl-KCl-$CaCl_2$-H_2O systems by Raman spectra and found that anions interacted with water molecules on the hydrogen donor side of the molecule, whereas cations interacted through lone pairs (acceptor side) (Sun, Zhao, Li, & Liu, 2010). As a result, hydrogen bond interactions decreased correspondingly.

Furthermore, Raman bands near 1450 cm^{-1} and 2800-3000 cm^{-1} corresponded to C-H bending and stretching vibrations, respectively (Herrero et al., 2008). As shown in Fig. 2, the C-H bending and stretching vibrations of KGM were located at 1453.71 cm^{-1} and 2888.84 cm^{-1}, respectively, while KGM-KCl gel had stronger vibration intensities near 1381.74 cm^{-1} and 2899.8 cm^{-1}. This might be because methyl- or methylene groups of the KGM-KCl gel were exposed to the polar environment of the KCl solution. The changes in location, intensity and band area, which are assigned to the vibrations of the C-H bond, indicate changes in the environment of C-H groups, which may be related to hydrophobic interactions (Xu, Han, Fei, & Zhou, 2011). Larsson & Rand also reported that the intensity of the 2930 cm^{-1} band increased with increasing polarity of the environment around hydrocarbon chains (Larsson & Rand, 1973). In addition, the higher intensity of C-H stretching vibrations at 2899.8 cm^{-1} implied that the -CH hydrophobic groups of KGM in the gel were not exposed, which could be ascribed to the more compact gel structure (Xue, Qian, Kim, Xu, & Zhou, 2018). According to the above analysis, combined with experimental phenomena, we thought the main forces for gel formation and gel stability were electrostatic and hydrophobic interactions. These results all coincided with the FTIR analysis.

3.4 SEM observations

Fig. 3 shows SEM images of native KGM powder (a), lyophilized KGM hydrosol (b), KGM-AC (c-f) and lyophilized KGM-KCl gels (g-i) with different magnifications. KGM powder presented a regular microfibre shape with many short chain branches between the tightly arranged backbone chains. The microfibres were glued to each other, which might be due to intra- and intermolecular hydrogen bond formation between KGM molecules.

The bonds played an important role in stabilizing the microfibre chain structure of KGM (Fig. 3a).

The morphology of the freeze-dried KGM hydrosol is shown in Fig. 3b. KGM presented a disorganized flocculation instead of the original regular microfibre structure after freeze-drying. This was because water molecules bound and filled between KGM molecular chains by many intermolecular hydrogen bonds evaporated during vacuum freeze drying, leaving the swollen KGM molecular chain frozen and fixed in its original position to form a scaffold structure. In addition, some KGM micelles were thicker and some were thinner due to the strong interaction between KGM molecules, which was caused by hydrogen bonds.

Distinct changes were found in the morphology of KGM-AC compared with that of KGM powder and lyophilized KGM hydrosol. As shown in Fig. 3 (c-f), the regular microfibres of KGM and its scaffold structure disappeared. Instead, KGM presents a flaky and uneven layered structure. This was because KGM microfibres were fractured under AC electric field treatment, and short KGM molecular chains could not wrap water molecules to form scaffold structures. The results were in accordance with the analysis of FTIR and Raman spectra. In addition, it can be seen from the image with high magnification (Fig. 3f) that there are obvious breaking of KGM molecular chains. We also found that the lyophilized KGM hydrosol treated by an AC electric field was fragmented into several pieces with different sizes rather than a whole piece of sponge-like product by experimental observations.

Fig. 3 (g-i) shows the morphological structure and surface images of AC electric field-induced KGM-KCl gels. It can be seen from the SEM photographs that KGM-KCl electrogels exhibited a porous structure, allowing the gel to maintain certain elastic characteristics. It possessed a rough and irregular surface with many folds. The walls of the gels were coarse, and the pore size distribution was not homogeneous.

3.5. Steady shear measurements of KGM sols and KGM-KCl mixed sols

To explore the effect of the AC electric field on the molecular chains of KGM, steady shear measurements were conducted. Apparent viscosities of KGM sols and KGM-KCl complex hydrosols without and with electric treatment were recorded on an advanced AR-2000 ex rheometer. The mixed sol was treated for 25 min by applying an AC electric field to not form a gel. In addition, according to our knowledge, the formation of electrogel is a process of aggregation of KGM molecules between electrodes; thus, the homogeneous KGM-KCl sol becomes a nonuniform system after electroprocessing for a certain time. Therefore, KGM composite sols for determination were sampled from different points, including from the centre of the beaker, from the vicinity of the beaker wall and from the vicinity of the electrode. The flow curves are presented in Fig. 4. From Fig. 4, we can see that the apparent viscosities of all the samples, including KGM sol and KGM-KCl mixtures with and without electric treatment, all decreased as the shear rate increased, demonstrating that the sols exhibited non-Newtonian fluid properties (Ma, Zhu, & Wang, 2019). Furthermore, the apparent viscosities of the KGM sol (Fig. 4a) and KGM-KCl mixture (Fig. 4b) treated by an AC electric field were all lower than that of the sol without electric treatment, indicating the breaking of KGM molecular chains after electric treatment in water or KCl solution (Tatirat, Charoenrein, & Kerr, 2012). That is, AC electric field treatment was found to be able to reduce KGM solution viscosity in a simple and controllable manner, and it could be an effective degradation method for KGM and other polysaccharides. This result was in good agreement with the findings from the FTIR, Raman and SEM analyses.

3.6. Frequency sweep

3.6.1. Effect of KCl concentration on G′ and G″ of KGM-KCl gel

To explore the optimum conditions for preparing KGM-KCl electrogel, the effects of four factors, including KCl concentration, electric treatment time, voltage and KGM concentration, on the rheological properties of the gels were studied. First, considering the importance of KCl in gel formation, we studied the effect of KCl concentration on the rheological properties of the gels. To examine the frequency dependence of G′ and G″ of the KGM-KCl electrogel, frequency sweep tests were carried out using small amplitude oscillatory shear. As shown in Fig. 5a, in the high frequency area, G′ and G″ of the gels increase only slightly with frequency, suggesting the formation of a good gel network structure in the samples. This slight increase also indicated their abilities to resist external deformation (Wang, Jiang, Lin, Pang, & Liu, 2016). In addition, the elastic modulus (G′) of all the samples prepared with different concentrations of KCl dominates the viscous modulus (G″), which indicates the gel-like nature of the products (Li, Ye, Zhou, Lei, & Zhao, 2019). By comparing the changes in moduli of the gels prepared with different concentrations of KCl (c_k), we found that when c_k increased from 0.5% to 0.7%, G′ and G″ increased. This might be because the adsorption of chloride ions on the -OH groups of KGM molecules depends on chloride ion concentrations. As the concentration of Cl^- ions increases, more adsorption occurs (Bagheri, Nazari, Sanjayan, & Duan, 2018). KGM was more charged with more KCl due to the adsorption of K^+ and Cl^- ions, and thus, the charged KGM molecular chains interpenetrated each other to form network structures under an AC electric field. When c_k was 0.7%, the KGM sol started to boil in the last few minutes of AC electric field processing. Under this circumstance, the gel could still form. The moderate boil not only caused the gel to form at the gas/liquid interface but could also remove some of the gases from the gel. Therefore, the moduli of the gels were relatively higher. However, G′ and G″ decreased when c_k exceeded 0.7%. This was because the greater the amount of KCl added, the greater the heat release during the application of the AC electric field. As a result, on the one hand, KGM molecular chains broke severely under high temperature. On the other hand, the high heat and temperature destroyed the stability of the formed gel. When c_k was above 0.9%, it was no longer possible to produce gels. This was because the added KCl was too much, and KGM sol boiled too violently to form the gel. The whole gelation process reflected the vital role of KCl and its suitable concentration in gel formation. Therefore, we chose a concentration of 0.7% KCl.

3.6.2. Effect of electric processing time on G′ and G″ of KGM-KCl gel

Second, to explore the importance of the application of an AC electric field on gel formation, we studied the influence of electric processing time on the rheological properties of KGM-KCl gels. The results are shown in Fig. 5b. When an AC electric field was applied for 35 min, the gel formed. Notably, no gel formed when the electric treatment time was less than 35 min. It can be seen from Fig. 5b that when the electric treatment time is increased from 40 min to 50 min, G′ and G″ correspondingly increase with G′ being larger than G″. This is probably because when the voltage, KCl concentration and KGM concentration are fixed, the time needed for the intercutting of KGM molecular chains extends with the increase of electric treatment time, resulting in the formation of a more compact gel network. When the electric treatment time was increased from 50 min to 60 min, G′ and G″ correspondingly decreased, indicating a decrease in gel strength. When the electric treatment time exceeded 60 min, the formed gel dissolved. This might be because as the electric processing time extended, the stability of the

gel decreased under the high temperature caused by the heat release, which was generated by the movement of ions. From the above, KGM-KCl electrogel can form in at least 35 min of electric treatment. This differs from our previous reports about the preparation of KGM-tungsten electrogels, which can form in 3 min of DC electric processing (Wang, Jiang, Lin, Pang, & Liu, 2016; Wang, Zhuang, Li, Pang, & Liu, 2016). These experiments highlighted the importance of the application of an AC electric field in KGM-KCl electrogel formation. Therefore, an electric treatment time of 50 min was chosen in the following experiments.

3.6.3. Effect of voltage on storage modulus (G′) and loss modulus (G″) of KGM-KCl gel

The effect of voltage on the rheological properties of KGM-KCl gels is shown in Fig. 5c. As shown in the figure, voltage significantly affected the rheological properties of the gels. As the voltage increased by 1 V, the G′ and G″ of the gels changed greatly, and the effect of the voltage was similar to the effects of KCl concentration and electric treatment time. In particular, when the voltage increased from 21 V to 23 V, G′ and G″ of the gel increased, with G′ being larger than G″. This might be because with increasing voltage, the electric field strength increased and the movement of the charged KGM molecular chains accelerated, resulting in more intercutting of KGM chains under a fixed electric processing time; thus, the strength of the formed gel increased. However, when the voltage increased from 23 V to 25 V, G′ and G″ of the gel decreased. This might be because the motion of some unadsorbed K^+ and Cl^- ions strengthened under high electric field strength, resulting in substantial heat release, which reduced the stability of the formed gel. On the other hand, KGM molecular chains broke more severely under high temperatures, as we mentioned above, and under high electric field strength, which has been verified by SEM observations and steady shear measurements. When the voltage was below 21 V or exceeded 25 V, no gel appeared. This might be because either the electric current was too low to drive the motion and entanglement of charged KGM molecular chains or because the electric current and heat released were too high to form the gel. Additionally, a higher voltage could lead to the KGM sol boiling violently. The effect of the voltage on the moduli of the gels and the gel formation suggested that the application of an appropriate voltage was critical to the formation and stability of a gel. This finding also indicated that AC electric treatment was one of the necessary conditions for the formation of the electrogel. Therefore, we chose 23 V as the voltage in the following experiments.

3.6.4. Effect of KGM concentration on G′ and G″ of KGM-KCl gel

Finally, the effect of KGM concentrations (c_{KGM}) on G′ and G″ of KGM-KCl electrogels was studied. The results are presented in Fig. 5d. It can be seen from Fig. 5d that G′ and G″ of the KGM-KCl gel increase with increasing c_{KGM} from 0.5% to 1.1%. This might be because with increasing c_{KGM}, the number of charged KGM molecules involved in interpenetrating and tangling with each other increases. When c_{KGM} reached 1.3%, the KGM sol became thicker, and the mobility of KGM molecular chains was affected. Therefore, we did not prepare the gel at a 1.3% concentration of KGM. The trend of the dependence of G′ and G″ on KGM concentration was opposite to that of KGM-tungsten gels we reported earlier (Wang, Jiang, Lin, Pang, & Liu, 2016) because the gelation mechanism of KGM-KCl and KGM-tungsten electrogels was different. For KGM-KCl gels, the charged KGM molecules due to the adsorption of K^+ and Cl^- ions on -OH groups of KGM molecules are the key to forming the gel, while for KGM-tungsten gels, isopoly-tungstic acid ions generated from the transformation of WO_4^{2-} ions cross-link with -OH groups at the C-6 position on KGM under a DC electric field to form a

three-dimensional network. Thus, the ratio of isopolytungstic acid ions to KGM is critical to the formation and stability of the gel. Therefore, a concentration of 1.1% KGM was chosen for preparing KGM-KCl gel.

It has been reported that gels could form at least 0.5% c_{KGM} in NaOH solution (Luo, He, & Lin, 2013), and for KGM/borax gel, the lowest concentration of KGM studied was also 0.5% (Gao, Guo, & Nishinari, 2008). In our previous publications, gels could form at only 0.3% c_{KGM} in the presence of sodium tungstate under a DC electric field (Wang, Jiang, Lin, Pang, & Liu, 2016; Wang, Zhuang, Li, Pang, & Liu, 2016). In this research, we obtained gels at 0.5% c_{KGM} in the presence of KCl under an AC electric field. This indicates that the application of an AC electric field can also promote gel formation at almost the same low KGM concentrations.

Two Chinese patents, namely, CN101328222A and CN101328224A, have been approved for the preparation of *licorice and choerospondiatis* polysaccharide-metal complexes. The metal compounds include Na_2WO_3, Na_2SeO_4, $FeCl_2$, $CaCl_2$, and KCl, among others. The FTIR spectra of the complexes were also analysed. The results showed that the compounds had the same spectral characteristics as the native polysaccharides. Their characteristic peaks were at 3423-3419 cm^{-1}, 2926-2847 cm^{-1}, 1607-1621 cm^{-1}, 1159-1132 cm^{-1} and 1098-1015 cm^{-1}, which corresponded to the vibrations of -OH, $-CH_2$, -C=O, -C-O-C and -C-O-H, respectively. They also had the characteristic absorption peaks of β- and α- pyranose. However, the preparation method was more time-consuming, complicated, and labourious. It included filtering, dialysis, condensation, alcohol precipitation, sedimentation, washing, drying, etc. Finally, pure polysaccharide-metal materials were obtained.

In contrast, gel formation by applying an AC electric field is a much simpler, faster and more effective, controllable and adjustable method. It just requires an electrical current, electric field strength (i.e., voltage and the distance between the electrodes), KCl and KGM concentrations. Gel formation does not require heating. Gels can be obtained at a low concentration of 0.5% KGM with the aid of KCl without adding alkali and other substances. In addition, the gels form under high temperature circumstances, which endows the gels with high thermal stabilities. Compared with the method of DC induction, the use of AC can overcome serious electrolytic hydrolysis and electrochemical corrosion. Gel formation induced by AC requires only nontoxic KCl, without the help of toxic sodium tungstate. The effect of voltage on the formation of KGM-KCl gel induced by AC is greater than that of KGM-tungsten induced by DC (Wang, Jiang, Lin, Pang, & Liu, 2016; Wang, Zhuang, Li, Pang, & Liu, 2016). A small change in voltage can affect the formation of KGM-KCl gel and its moduli. However, it takes a longer time for the KGM-KCl electrogel to form under the AC electric field because the formation mechanisms of the two kinds of gels are different. In addition, AC can cause the KGM molecular chains to break, so the gel formed is relatively small and thin, while DC does not cause the KGM molecular chains to break. In the future, the adsorption properties, dielectric properties, electrochemical properties, mechanical properties and other properties of these two kinds of gels should be studied and compared.

3.7 The formation mechanism of the KGM-KCl electrogel

Based on the above experiments and analysis, we summarized that the formation mechanism of the KGM-KCl electrogel was as follows: K^+ and Cl^- ions adsorb on the hydroxyl groups of KGM molecular chains, and the charged KGM molecular chains run through each other to form a topological entanglement structure between the two electrodes under an AC electric field. Meanwhile, the number of interlocking molecules per unit volume increases due to the breakage of KGM molecular chains under AC. In addition, the AC electric field

promotes the ordered orientation of the KGM molecular chain parallel to the direction of the electric field. Electrostatic and hydrophobic interactions are the main driving forces for gel formation, rather than hydrogen bonds. A schematic representation of the formation mechanism of the gel is shown in Fig. 6.

Conclusion

In this study, KGM-KCl electrogels were successfully prepared at 0.5% KGM in the presence of KCl under an AC electric field. The FTIR, Raman and SEM characterization and rheological properties of the gels were studied, and the formation mechanism was summarized. The results showed that the AC electric field did not change the chemical main chain structure of KGM or produce new functional groups. KGM partially deacetylated under an AC electric field due to the hydroxide ions resulting from electrolytic hydrolysis. In addition, KGM molecular chains broke under an AC electric field and high temperature. The gels retained some characteristic acetyl groups of KGM molecules and possessed an ununiform porosity structure. The storage and loss moduli of KGM-KCl gels were found to increase when the KCl concentration, KGM concentration, voltage and electric processing time increased but decrease when the KCl concentration, voltage and electric processing time exceeded critical points. KGM and KCl interacted with each other to form the structure of 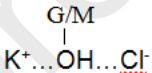

. Thus, the charged KGM inter-penetrated or tangled with each other to form the gel network with the application of an AC electric field. This novel electrogel will have potential applications in food, material engineering, chemical industries, etc.

Acknowledgments

This study was supported by the Doctor Scientific Research Foundation of Putian University (2019022), National Natural Science Foundation of China (31801462), Research and Innovation Projects of Putian University (2018ZP03), the Education and Research Project of Young and Middle-aged Teachers of Fujian Province (JT180467), and the Cultivation Program for the Outstanding Young Scientific Research Talents of Fujian Province (2018).

References

Bagheri, A., Nazari, A., Sanjayan, J. G., & Duan, W. H. (2018). Molecular simulation of water and chloride ion diffusion in nanopores of alkali-activated aluminosilicate structures. *Ceramics International, 44*, 20723-20731.

Brenner, T., Tuvikene, R., Fang, Y. P., Matsukawa, S., & Nishinari, K. (2015). Rheology of highly elastic iota-carrageenan/ kappa-carrageenan/ xanthan/ konjac glucomannan gels. *Food Hydrocolloids, 44*, 136-144.

Chen, Z., Yang, Y. L., Chen, F., Qing, Q., Wu, Z. Y., & Liu, Z. F. (2005). Controllable Interconnection of Single-Walled Carbon Nanotubes under AC Electric Field. *The Journal of Physical Chemistry. B, 109 (23)*, 11420-11423.

Gao, S. J., Guo, J. M., & Nishinari, K. (2008). Thermoreversible konjac glucomannan gel crosslinked by borax. *Carbohydrate Polymers, 72*, 315-325.

Herrero, A., Carmona, P., Cofrades, S., & Jiménez-Colmenero, F. (2008). Raman spectroscopic determination of structural changes in meat batters upon soy protein addition and heat treatment. *Food Research International, 41(7)*, 765-772.

Hermanson, K. D., Lumsdon, S. O., Williams, J. P., Kaler, E. W., & Velev, O. D. (2001). Dielectrophoretic

Assembly of Electricly Functional Microwires from Nanoparticle Suspensions. *Science, 294*, 1082-1086.

Jian, W. J., Siu, K. C., & Wu, J. Y. (2015). Effects of pH and temperature on colloidal properties and molecular characteristics of Konjac glucomannan. *Carbohydrate Polymers, 134*, 285-292.

Larsson, K., & Rand, R. P. (1973). Detection of changes in the environment of hydrocarbon chains by Raman spectroscopy and its application to lipid-protein systems. *Biochimica et Biophysica Acta (BBA) - Lipids and Lipid Metabolism, 326(2)*, 245-255.

Li, M. Y., Feng, G. P., Wang, H., Yang, R. L., Xu, Z. L., & Sun Y. M. (2017). Deacetylated konjac glucomannan is less effective in reducing dietary-induced hyperlipidemia and hepatic steatosis in C57BL/6 mice. *Journal of agricultural and food chemistry, 65(8)*, 1556-1565.

Li, X. J., Ji, N., Li, M., Zhang, S. L., Xiong, L., & Sun, Q. J. (2017). Morphology and structural properties of novel short linear glucan / protein hybrid nanoparticles and their influence on the rheological properties of starch gel. *Journal of Agricultural and Food Chemistry, 65 (36)*, 7955-7965.

Li, J. W., Ma, J. W., Chen, S. J., He, J. M., & Huang, Y. D. (2018). Characterization of calcium alginate/ deacetylated konjac glucomannan blend films prepared by Ca^{2+} crosslinking and deacetylation. *Food Hydrocolloids, 82*, 363-369.

Li, S. H., Ye, F. Y., Zhou, Y., Lei, L., & Zhao, G. H. (2019). Rheological and textural insights into the blending of sweet potato and cassava starches: in hot and cooled pastes as well as in fresh and dried gels. *Food Hydrocolloids, 89*, 901-911.

Liu, W. Y., Wang, C. H., Ding, H. T., Shao, J. Y., & Ding, Y. C. (2016). AC electric field induced dielectrophoretic assembly behavior of gold nanoparticles in a wide frequency range. *Applied Surface Science, 370*, 184-192.

Luo, X. G., He, P., & Lin, X. Y. (2013). The mechanism of sodium hydroxide solution promoting the gelation of konjac glucomannan (KGM). *Food Hydrocolloids, 30*, 92-99.

Luo, Y. C., Teng, Z., Wang, X. G., & Wang, Q. (2013). Development of carboxymethyl chitosan hydrogel beads in alcohol-aqueous binary solvent for nutrient delivery applications. *Food Hydrocolloids, 31*, 332–339.

Ma, S. P., Zhu, P. L., & Wang, M. C. (2019). Effects of konjac glucomannan on pasting and rheological properties of corn starch. *Food Hydrocolloids, 89*, 234-240.

Mu, R. J., Wang, L., Du, Y., Yuan, Y., Ni, Y. S., Wu, C. H., & Pang, J. (2018). Synthesis of konjac glucomannan-silica hybrid materials with honeycomb structure and its application as activated carbon support for Cu(II) adsorption. *Materials Letters, 226*, 75-78.

Niu, Y. G., Xia, Q., Li, N., Wang, Z. Y., & Yu, L. L. (2019). Gelling and bile acid binding properties of gelatin-alginate gels with interpenetrating polymer networks by double cross-linking. *Food Chemistry, 270*, 223-228.

Parikka, K., Nikkila, I., Pitkanen, L., Ghafar, A., Sontag-Strohm, T., & Tenkanen, M. (2017). Laccase/TEMPO oxidation in the production of mechanically strong arabinoxylan and glucomannan aerogels. *Carbohydrate Polymers, 175*, 377-386.

Sam, M., Moghimian, N., & Bhiladvala, R. B. (2016). Field-directed chaining of nanowires: towards transparent electrodes. *Materials Letters, 163*, 205-208.

Sun, Q., Li, G., Dai, L., Ji, N., & Xiong, L. (2014). Green preparation and characterisation of waxy maize starch

nanoparticles through enzymolysis and recrystallisation. *Food Chemistry, 162*, 223-228.

Sun, Q., Zhao, L., Li, N., & Liu, J. (2010). Raman spectroscopic study for the determination of Cl^- concentration (molarity scale) in aqueous solutions: application to fluid inclusions. *Chemical Geology, 272*, 55-61.

Tatirat, O., Charoenrein, S., & Kerr, W. L. (2012). Physicochemical properties of extrusion-modified konjac glucomannan. *Carbohydrate Polymers, 87*, 1545-1551.

Wang, L. X., Jiang, Y. P., Lin, Y. H., Pang, J., & Liu, X. Y. (2016). Rheological properties and formation mechanism of DC electric fields induced konjac glucomannan-tungsten gels. *Carbohydrate Polymers, 142*, 293-299.

Wang, W. J., Shen, M. Y., Liu, S. C., Jiang, L., Song, Q. Q., Xie, J. H. (2018). Gel properties and interactions of Mesona blumes polysaccharide-soy protein isolates mixed gel: The effect of salt addition. *Carbohydrate Polymers, 192*, 193-201.

Wang, H. Y., Wan, L., Chen, D., Guo, X. F., Liu, F. X., & Pan, S.Y. (2019). Unexpected gelation behavior of citrus pectin induced by monovalent cations under alkaline conditions. *Carbohydrate Polymers*, 212, 51-58.

Wang, K., Wu, K., Xiao, M., Kuang, Y., Corke, H., Ni, X. W., & Jiang, F. T. (2017). Structural characterization and properties of konjac glucomannan and zein blend films. *International Journal of Biological Macromolecules, 105*, 1096-1104.

Wang, Y. X., Wu, K., Xiao, M., Riffat, S. B., Su, Y. H., & Jiang, F. T. (2018). Thermal conductivity, structure and mechanical properties of konjac glucomannan/starch based aerogel strengthened by wheat straw. *Carbohydrate Polymers, 197*, 284-291.

Wang, X., Xiong, Y. L. L., & Sato, H. (2017). Rheological enhancement of pork myofibrillar protein-lipid emulsion composite gels via glucose oxidase oxidation/transglutaminase cross-linking pathway. *Journal of Agricultural and Food Chemistry, 65 (38)*, 8451-8458.

Wang, L. X., Zhuang, Y. H., Li, J. L., Pang, J., & Liu, X. Y. (2016). The textural properties and microstructure of konjac glucomannan-tungsten gels induced by DC electric fields. *Food Chemistry, 212*, 256-263.

Wang, S. S., Zhou, B., Wang, Y. T., & Li, B. (2015). Preparation and characterization of konjac glucomannan microcrystals through acid hydrolysis. *Food Research International, 67*, 111-116.

Xu, X. L., Han, M. Y., Fei, Y., & Zhou, G. H. (2011). Raman spectroscopic study of heat-induced gelation of pork myofibrillar proteins and its relationship with textural characteristic. *Meat Science, 87(3)*, 159-164.

Xue, S. W., Qian, C., Kim, H. Y. B., Xu, X. L., & Zhou, G. H. (2018). High-pressure effects on myosin in relation to heat gelation: A micro-perspective study, *Food Hydrocolloids, 84*, 219-228.

Ye, S. X., Jin, W. P., Huang, Q., Hu, Y., Li, Y., Li, J., & Li, B. (2017). Da-KGM based GO-reinforced FMBO-loaded aerogels for efficient arsenic removal in aqueous solution. *International Journal of Biological Macromolecules, 94*, 527-534.

Zhang, Y. Q., Xie, B. J., & Gan, X. (2005). Advance in the applications of konjac glucomannan and its derivatives, *Carbohydrate Polymers, 60*, 27-31.

Zhang, M., Yang, X., Zhou, Z. Y., & Ye, X. Y. (2013). Controllable growth of gold nanowires and nanoactuators via high-frequency AC electrodeposition. *Electrochemistry Communications, 27*, 133-136.

Zhang, K. G., Yang, W. Z., Xu, B., Chen, Y., Yin, X. S., Liu, Y., & Zuo, H. Z. (2018). Inhibitory effect of konjac

glucomanan on pitting corrosion of AA5052 aluminium alloy in NaCl solution, *Journal of Colloid and Interface Science, 517*, 52-60.

Zhu, F. (2018). Modifications of konjac glucomannan for diverse applications. *Food Chemistry, 256*, 419-426.

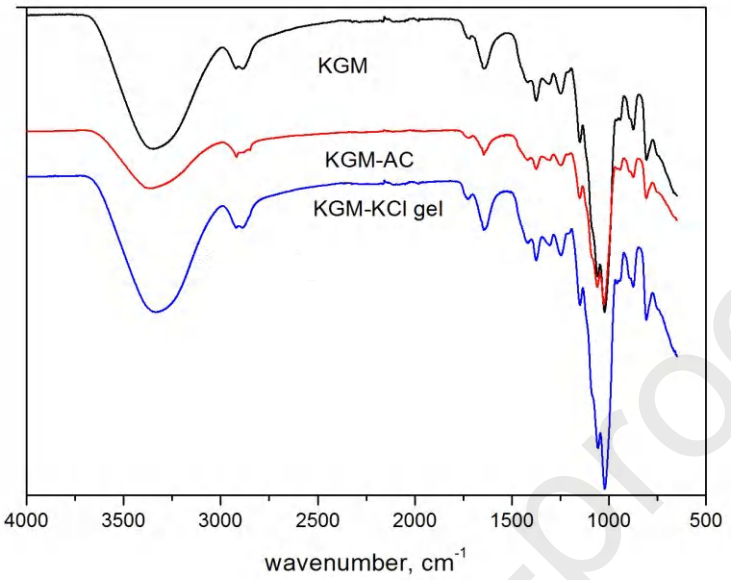

Fig. 1 FTIR spectra of native KGM, KGM-AC and KGM-KCl gel

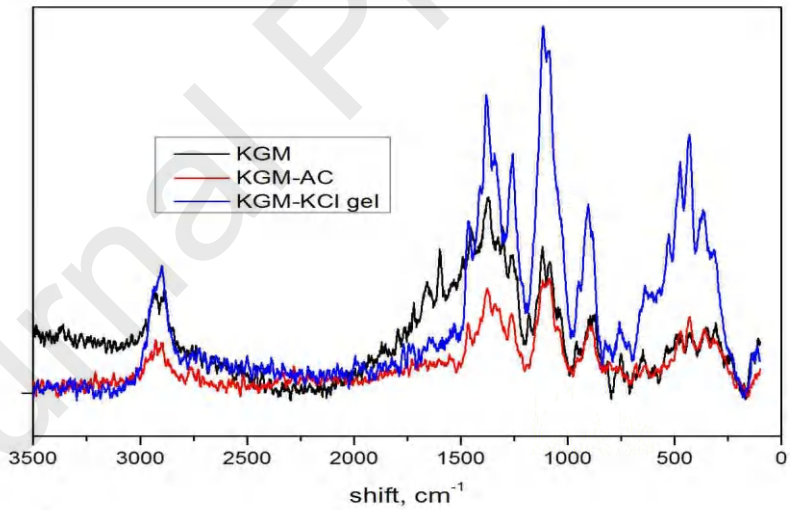

Fig. 2 Raman spectra of KGM, KGM-AC and KGM-KCl gel

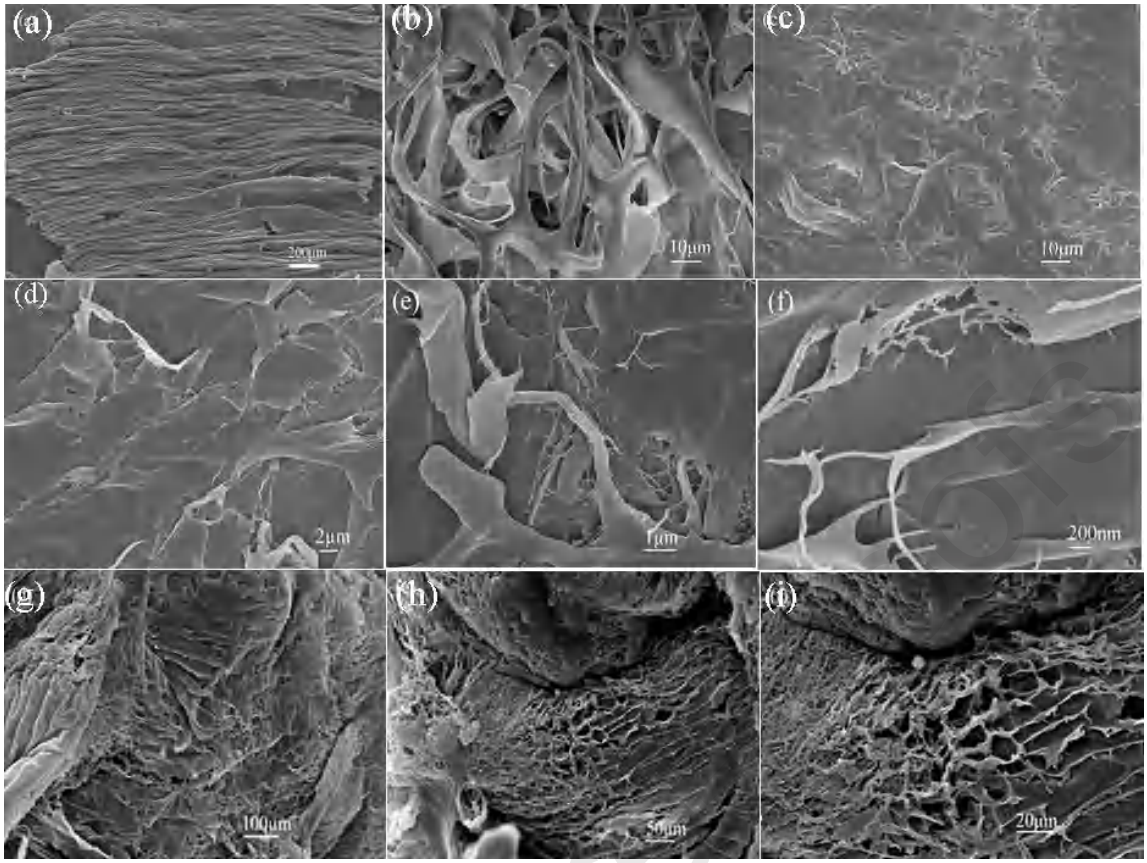

Fig. 3 SEM images of native KGM powder (a), lyophilized KGM hydrosol (b), KGM-AC (c-f) and lyophilized KGM-KCl gels (g-i) with different magnifications

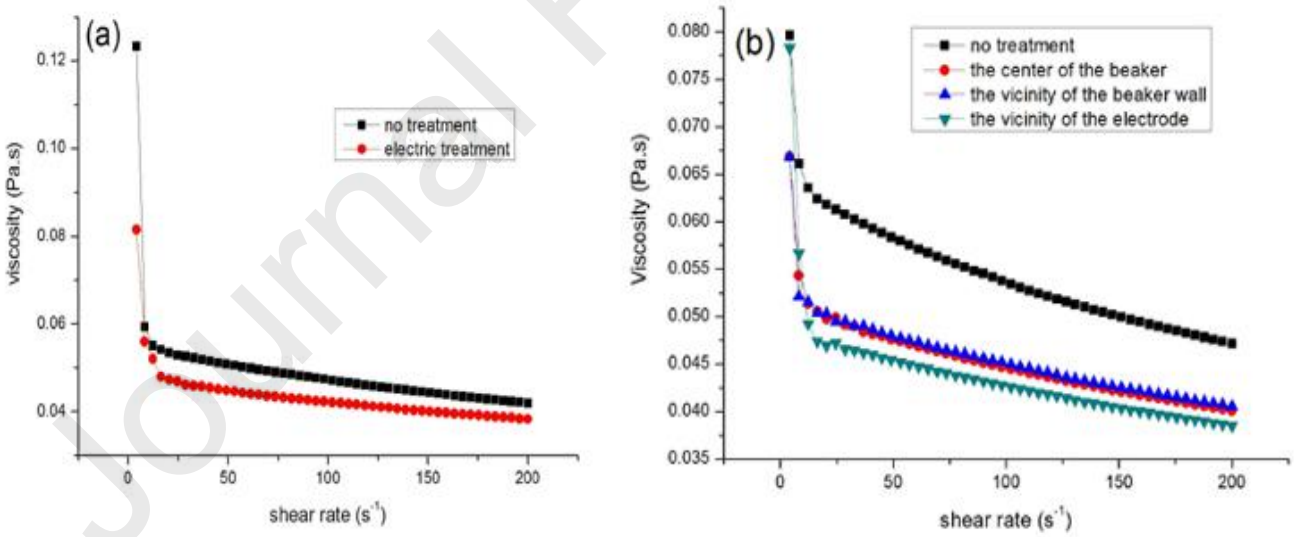

Fig. 4 Effect of an AC electric treatment on the apparent viscosity of KGM sols (a) and KGM-KCl mixed sols (b), a represents 0.5% KGM sol without and with electric treatment time for 30 min at 25 V, b represents 0.5% KGM sol containing 0.7% KCl without and with electric treatment time for 25 min at 25V

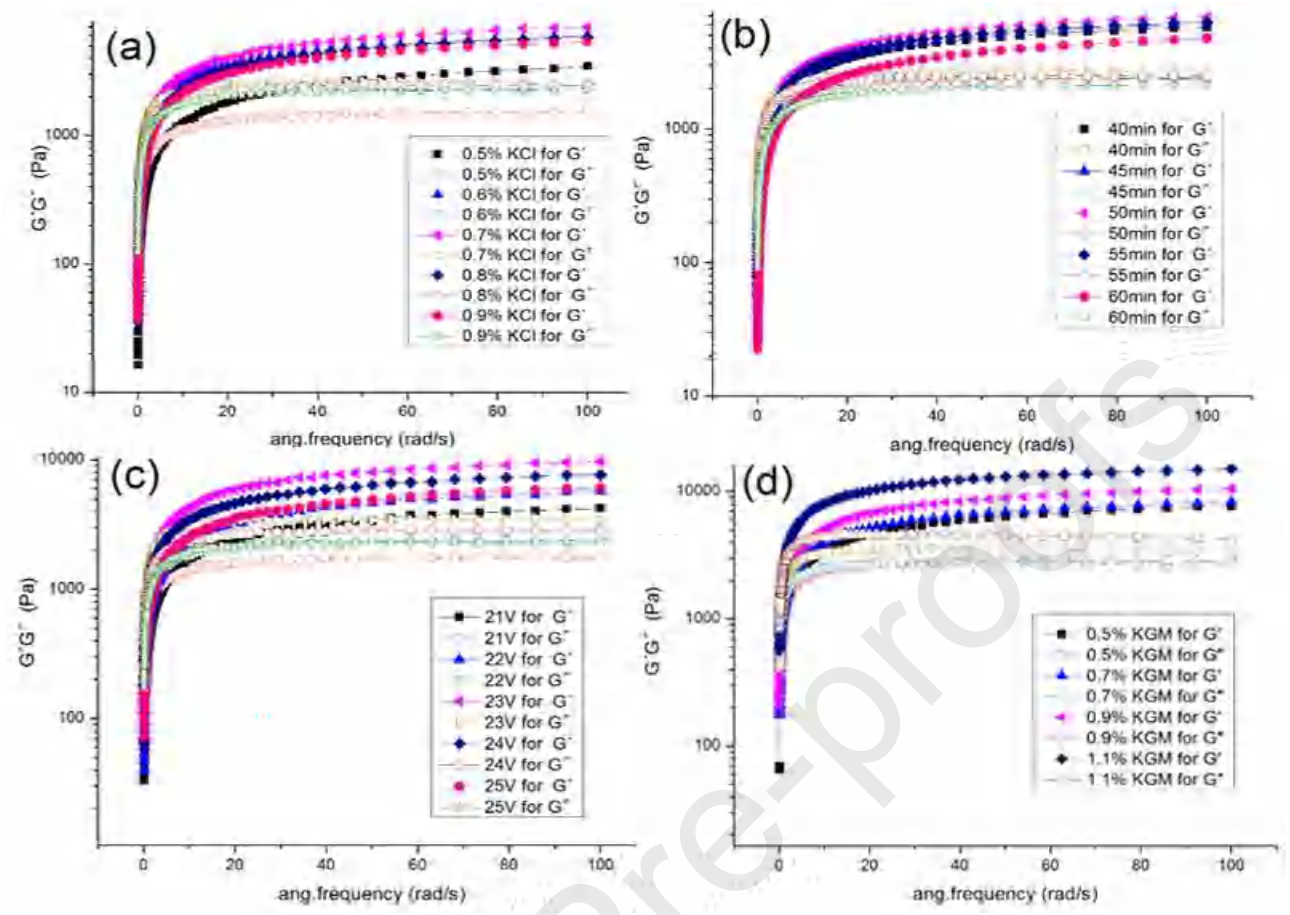

Fig.5 Frequency dependence of G′ (full symbols) and G″ (open symbols) for KGM-KCl gels (a: different KCl concentration, c_{KGM}: 0.5%, voltage: 25V, time: 40min; b: different electric treatment time, c_{KGM}: 0.5%, c_K: 0.7%, voltage: 25V; c: different voltage, c_{KGM}: 0.5%, c_K: 0.7%, electric treatment time: 50min; d: different KGM concentration, c_K: 0.7%, electric treatment time: 50min, voltage: 23V)

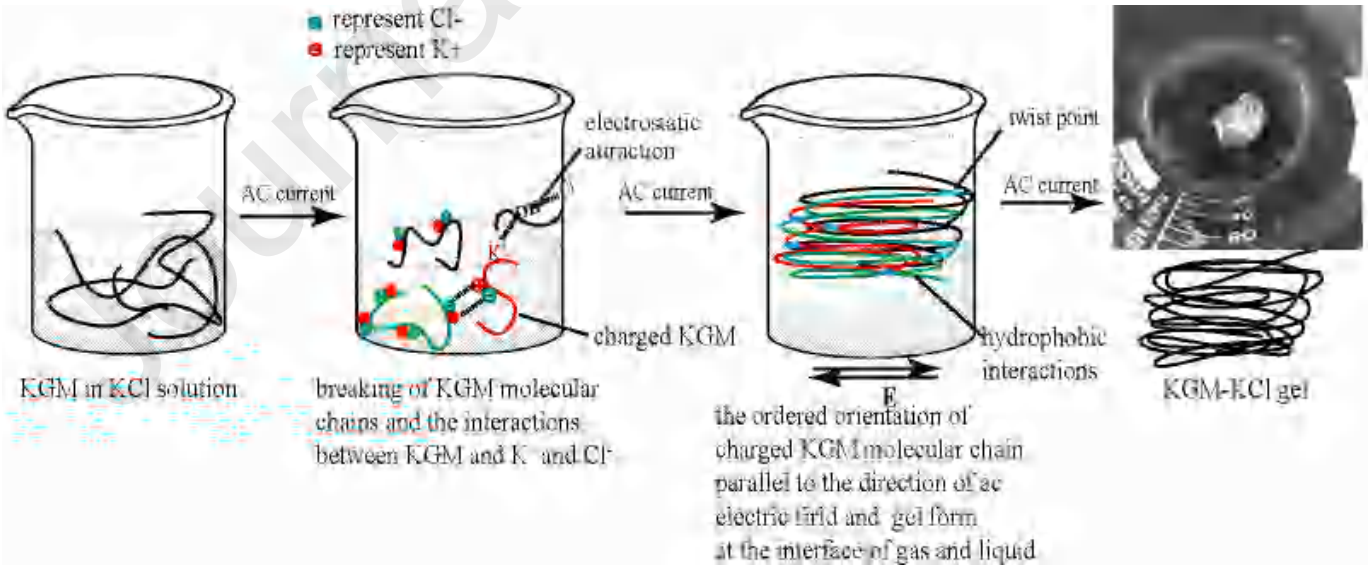

Fig. 6 Schematic representation of the formation mechanism of KGM-KCl electrogel

Ting-Jang Lu: corresponding author, ensure that the descriptions are accurate and agreed by all authors.

Li-Xia Wang: Conceptualization, Methodology, Validation, Formal analysis, Investigation, Writing - Original Draft, Writing - Review & Editing, Visualization.

Anng-Ruei Lee: Investigation.

Yi Yuan: Investigation.

Xiu-Mei Wang: Investigation, Funding acquisition.

1.Potassium chloride interacts with hydroxyl groups of konjac glucomannan to form the structure of 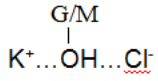

.

2.Konjac glucomannan molecular chains break and partially deacetylate under alternating current electric field.

3.Alternating current induces the formation of konjac glucomannan-potassium chloride electrogel.

4.Konjac glucomannan-potassium chloride electrogel possesses an ununiform porosity structure.

5.Viscoelastic moduli of the gels depend on potassium chloride and konjac glucomannan concentration, voltage and electric processing time.